Journal of Electron Devices, Vol. 18, 2013, pp. 1531-1536

© JED [ISSN: 1682 -3427]

Journal of Electron Devices
www.jeldev.org

High Frequency Noise Performance of Optically Controlled MOSFET

Prerana Jain[1], B.K. Mishra[2]
[1] SKVM's NMIMS, Mumbai, India. [2] T.C.E.T./Principal, Mumbai, India.
jainpnj@gmail

Received 11-07-2013, online 25-08-2013

ABSTRACT Noise model for optically controlled MOSFET is developed, valid for frequency range upto 10 GHz. The complete set of parameters used to characterize high frequency noise is computed under dark condition and under optical illumination. The noise analysis indicates reduction of noise under incident light, indicating the device application as low noise photodetector and in optoelectronic applications for high frequency system design.

***Index Terms*:** Modelling, MOSFET, Noise parameters, Optoelectronics, Photodetector, RF

I. INTRODUCTION

CMOS technology, the most economical and mature technology has already proven its capacity to work at RF. The speed of present submicron device circuits is restricted by electrical interconnects rather than device limitations [1]. One of the option is to replace critical path electrical interconnect with optical interconnect. Hence development of CMOS compatible photodetector is the need of existing technology. Control of the CMOS compatible device by optical illumination offers additional control port with the advantages of reliability, immunity to electromagnetic interference etc [2]. Performance of OG-MOSFET at RF is an important issue and is characterized by transit frequency f_t, maximum frequency of oscillation f_{max}, and minimum noise figure NF_{min}. These figures of merit for optically controlled MOSFET are already analysed in [3]. Low noise is one of the prime requirements of the photodetector. In addition to these figures of merit, a complete noise analysis is vital in deciding overall characteristics of the system [4]. There are several noise sources contributing to total noise at RF. It has been discussed that dominant noise contribution at high frequency is due to channel thermal noise and hence is considered for the present analysis [5].

The paper is structured as follows. Section II presents the MOSFET under illumination. Section III describes the theory related to noise in MOSFET and its modelling. The results and the discussion form section IV.

II. MOSFET UNDER ILLUMINATION

The device operation at RF requires the conventional MOSFET structure to be modified. A multifinger MOSFET structure with small finger width is under consideration so as to achieve reduced gate resistance. The single finger device structure of n-channel MOSFET with ion implanted profile under consideration is as shown in Figure 1.

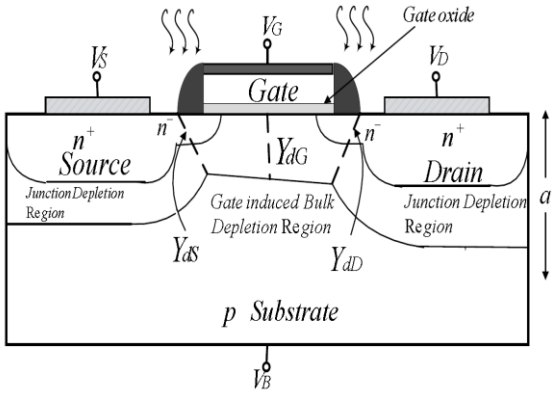

Figure 1: Schematic of MOSFET under illumination

This device is subjected to optical radiation, which is assumed perpendicular to the surface and the wavelength of radiation is higher than that of silicon bandgap energy of 1.12 eV. The incident wavelength considered is 830 nm so that the device can be used in short-haul communication and for chip to chip interconnect.

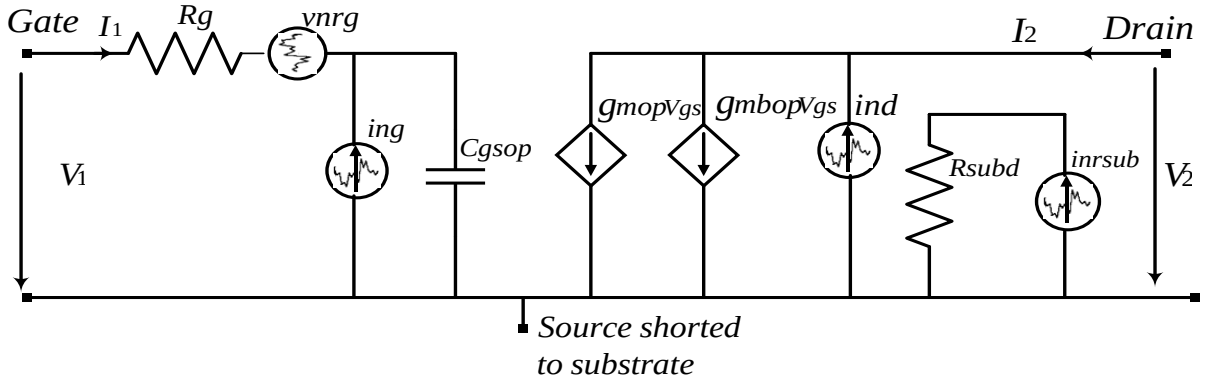

Figure 2: Equivalent noise model of MOSFET under illumination

When the MOSFET with the opaque polysilicon gate is illuminated, intrinsic absorption of the optical signal takes place within the inter-electrode spacing that is in the gate-source and the gate-drain region in the space charge region and also in the substrate. This absorption process causes generation of electron-hole pairs, which increases the minority carrier concentration and generation of charges which produce photo-voltage [6].

The channel profile of the MOSFET gets modified under illumination. It is essential to consider the additional charges due to illumination ($Q_{illumination}$) in order to calculate the total inversion charge under optical [7]. The carriers are generated in depletion region (Q_{dep1}) and the neutral region ($Q_{neutral}$) under optical illumination. These additional charges due to optical generation are evaluated by applying suitable boundary conditions. The charges generated due to illumination are as:

$$Q_{illumination} = Q_{neutral} + Q_{dep1} \quad (1)$$

Thus the total inversion charge under illumination will be as:

$$Q_{total} = Q_{inv} + Q_{illumination} \quad (2)$$

Thus change in inversion charge under illumination results in modification of gate, drain and bulk charge which modifies the device conductances and capacitances under illuminations. This changes the built in potential and causes increase in the inversion layer charges which results in change of channel conductivity. This will change the intrinsic parameters, effective threshold voltage and the channel resistance due to photoconductive and photovoltaic effect.

The calculation of photo-voltage is important as it the component which will be crucial in deciding the drain current. Photo-voltage is calculated from the current density. Continuity equation aids in evaluating current density.

The photo-voltage across the MOS diode is obtained using [7,8,9]

$$V_{op} = \frac{KT}{q} ln\left(\frac{J_p}{J_s}\right) = \frac{KT}{q}\left(\frac{qv_y.p(0)}{J_{S1}}\right) \quad (3)$$

where
K is Boltzman constant
q is electron charge
T temperature in Kelwin
Js_1 is the reverse saturation current,
v_y is the carrier along vertical direction perpendicular to the device surface,
Vop is the photo-voltage generated.

p(0) is the number of holes crossing junction at y=0,

$$p(0) = \frac{\Pi}{4} W(p_1 YdS^2 + p_2 YdD^2) \quad (4)$$

where p_1 and p_2 are constants dependant on carrier lifetime under ac conditions

Y_{dD} and Y_{dS} are depletion widths at drain and source respectively.

The generated photovoltage plays an important role as it modifies the depletion width. Using the abrupt junction approximation, under dark condition $Y_{dG}(x)$ as given by

$$Y_{dG}(x) = \left[\frac{2\varepsilon}{qN_{dr}}(\phi_{Bi} - \Delta + V_{ch}(x) - V_G)\right] \quad (5)$$

Under illumination due to photo-voltage developed at the gate, the gate voltage changes and the gate depletion width Y_{dG} gets modified to Y'_{dG} and is given by

$$Y'_{dG}(x) = \left[\frac{2\varepsilon}{qN_{dr}}(\phi_{Bi} - \Delta + V_{ch}(x) - V_G - V_{OP})\right] \quad (6)$$

where $V_{ch}(x)$ is the channel voltage,
ϕ_{Bi} is the built in potential of the n-p junction
ε is the permittivity,
Δ is the position of Fermi level at neutral region below conduction band
V_G is the gate potential.
Thus the drain current changes with the change in photo-voltage.

III. MOSFET MODELLING AT RF

The small signal model of MOSFET at RF essentially uses an equivalent sub-circuit approach. In a MOSFET, there are various noise sources. They include the terminal resistance thermal noise (at gate, source, drain and the substrate), thermal noise in the channel and the induced gate noise. Contribution of flicker noise in channel is neglected since it primarily affects the low frequency performance of the device and the interest of the present work is noise analysis at high frequency [10].

Thermal noise is the MOSFET is due to the random thermal motion of charge carriers. It affects the drain current noise spectrum, and is also due to the capacitive coupling between channel and gate [11]. This important noise which is from gate and substrate resistance is accounted in the existing approach. This paper presents complete high-frequency thermal noise models of short-channel MOSFETs, which includes the drain channel noise, the induced gate noise, and their correlation coefficients.

The circuit designers prefer to use the parameters related to two port network to describe the noise performance of a device and a circuit as in [12].

The noisy two port can be characterized by four parameters: the minimum noise figure (NF_{min}), the input-referred noise resistance (R_V), and the real and imaginary part of optimum source admittance(Y_{opt}). The real part is optimum source conductance (G_{opt}) and imaginary part is optimum source susceptance (B_{opt}).

The correlation relationship is described by correlation admittance (Yc).

$$Y_c = G_c + jB_c \quad (7)$$

The four correlation parameters characterizing the noise sources v_n and i_n of the noisy two port are R_{va}, Input-referred thermal noise current conductance (G_i),

noise correlation conductance (G_c) and noise correlation susceptance (B_c)[13].

The noise factor is a figure of merit for the performance of a device or a circuit with respect to noise. The standard definition of the noise factor of a two-port network is the ratio of the available output noise power per unit bandwidth to the portion of that noise caused by the actual source connected to the input terminals of the device. It is generally expressed in decibels. It can be given by (8,9)

$$F = \frac{S_i / N_i}{S_o / N_o} \tag{8}$$

$$N_F = 10 \log F \tag{9}$$

The noise figure *(NF)* is generally affected by two factors - the source (input) impedance at the input port of a network and the noise sources in the two-port network itself. The actual noise factor can be written as

$$F = F_{min} \frac{R_v}{G_s} \left[(G_s - G_{opt})^2 + (B_s - B_{opt})^2 \right] \tag{10}$$

$$Y_s = G_s + jB_s \tag{11}$$

$$Y_{opt} = G_{opt} + jB_{opt} \tag{12}$$

Where B_s is the source susceptance, Gs is the source conductance, G_{opt} is the optimized source conductance, B_{opt} is the optimized source susceptance, R_v is the input referred thermal noise resistance, Y_s is source admittance and Y_{opt} is optimized source admittance which is equivalent normalized noise resistance of the two port network. All the noise parameters and the correlating noise parameters are simulated using the expression given in [5,13] based on Appendix A .

In the circuit model under illumination for RF frequency, the MOSFET is biased in strong inversion and is in saturation. Due to this the output conductance g_{ds}, capacitances C_{bs} and C_{bd} have been neglected to calculate the noise parameters analytically .The capacitance C_{gsop} represents the gate to source capacitance under illumination including intrinsic and extrinsic parts. A single substrate resistance R_{sub} represents the all the substrate resistances. The g_{mop} and g_{mbop} represents the gate transconductance and bulk transconductance under illumination. The v_{nrg} corresponds to noise voltage source caused by polysilicon gate resistance R_G. i_d signifies the channel noise source occurring at high frequency. i_g is the induced gate noise occurring at high frequency. i_{nrsub} characterizes the noise source due to substrate resistance.

The capacitances, transconductances and the resistances in dark condition are evaluated by using the methodology and expressions in [14] and under illumination by using [15, 16].

IV. RESULTS AND DISCUSSIONS

The n-MOSFET device is a multifinger device with N_f =10, W_f= 12μm and L_f = 0.36μm. W_f and L_f are effective width and length of single finger. N_f is the number of fingers. The process parameters for simulation are 0.25 μm CMOS process, with oxide thickness t_{ox}=5.7 nm, V_{to}=0.55 V and substrate factor=0.466√V.

Numerical calculations are carried out to determine the photovoltage, the total channel charge and of the optically gated MOSFET for different illuminations for optical flux densities varying from Φ =1 x 10^{14} Wb/m^3 to Φ =1 x 10^{18} Wb/m^3. The calculations are done under DC and AC conditions for biasing potential of V_G=1 V, V_D=1 V and V_B=0 V at 300 K. The noise parameters are calculated analytically where the bias dependence is accounted for junction and overlap capacitances. The resistance values are considered bias independent. These calculations are done using the model equations developed using MATLAB.

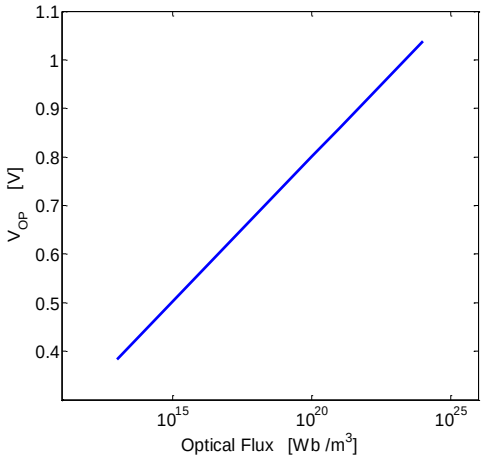

Figure 3: Optical voltage Vs optical flux density

Figure 3 is the change of optical voltage with variation in optical flux density. The optical flux increases logarithmically with optical power as per (3).

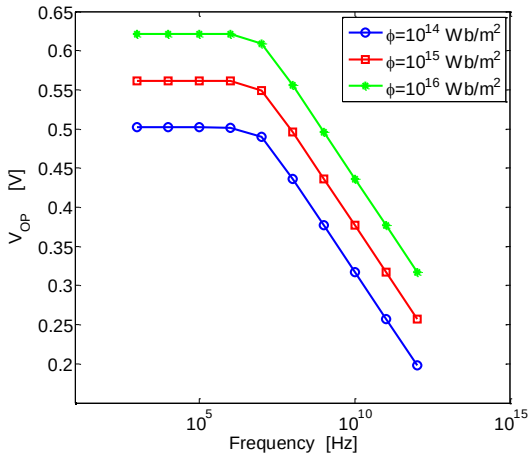

Figure 4: Optical voltage Vs frequency

Figure 4 indicates the variation of optical voltage against the variations in frequency for change in optical

flux density. It can be seen that the optical voltage is almost constant for frequency of about 100 MHz and the then falls gradually with increasing frequency. This is because the AC lifetime of carriers which are dependent on the signal frequency.

Figure 5 shows channel potential(V_{ch}), electric field(E), and inversion charge density(Q'_{inv}) variation along the channel in saturation region of MOSFET till the pinch-off point with $V_D = V_{Dsat}$ under dark and illumination. The potential distribution along the channel is an important parameter of the MOS device as it determines the electric field in the channel, mobile charge distribution, transit time, etc. It is found that the channel potential increases linearly near the source end (i.e. x/L=0) and becomes nonlinear near the drain end (x/L=1). This is because due to the fact electric field near the drain causes the conductivity to increase rapidly. Due to this it is expected that the electric field near the drain end reaches the critical field for high drain voltage and hence causes the velocity saturation. It can be seen that the channel pinch-off takes place earlier and the device reaches saturation sooner as compared to dark condition, which gets reflected in the drain current characteristics.

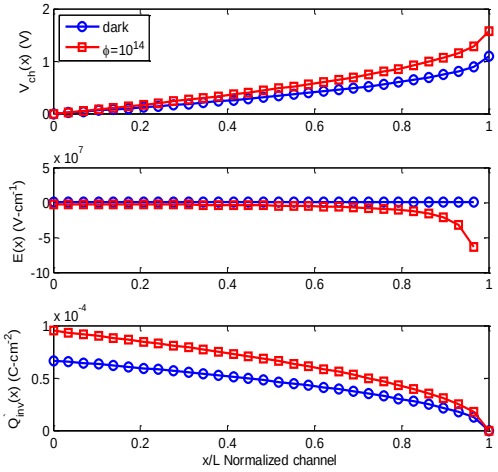

Figure 5: Channel potential, electric field, and inversion charge density variation along the channel

The distribution of electric field along the channel is depicted in the Figure 5 and for dark and illuminated condition respectively. In both the cases the electric field increases slowly near the source end and rapidly near the drain end. This is due to the fact that the carrier density near the drain end experiences a rapid decrease in surface concentration which calls for a rapid increase in the electric field to maintain the constant drain current. It is also seen that the electric field near the drain end in the illuminated condition is less compared to the value of the dark. As a result a high drain voltage is needed to attain saturation in the illuminated condition.

Figure 5 presents the magnitude of inversion charge density in dark and under illumination. The generation of electron-hole pair under illumination ($Q_{Illumination}$) in depletion and neutral regions contribute for rise in the total inversion charge which causes increase in drain current under illumination.

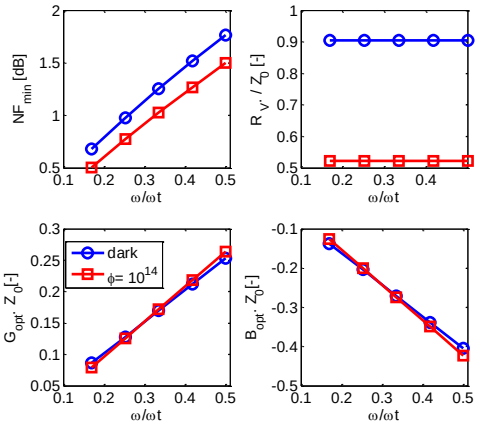

Figure 6: Minimum noise figure, input referred noise resistance, optimum source admittance (conductance and susceptance)

Figure 6 is the plot of minimum noise figure, optimum source admittance(conductance and susceptance) and input referred noise resistance in dark and under optical flux density with power of radiation Φ =1 x 10^{14} Wb/m^3. The transit frequency for operating point of V_G=1 V, V_D=1 V and V_S=0 V under dark condition is computed and taken as 18.67 GHz and under illumination for Φ =1 x 10^{14} Wb/m^3 is 22.79 GHz. The noise parameters of the device under illumination depend on the transconductance, gate to source capacitance and frequency of operation. The transconductance increases under illumination while there is reduction in magnitude of gate to source capacitance. The input referred noise resistance (R_v) is inversely proportional to the transconductance and hence is seen to decrease under illumination. The noise resistance is measure of how the noise figure increases as the source admittance moves away from the optimum source admittance. The source conductance and susceptance remain almost unchanged with optical illumination. Since the noise figure essentially depends on the product of noise resistance and source admittance, the noise figure is seen to decrease under optical illumination. It can be seen that the minimum noise figure is a frequency dependant parameter for the OG-MOSFET under dark and under illumination.

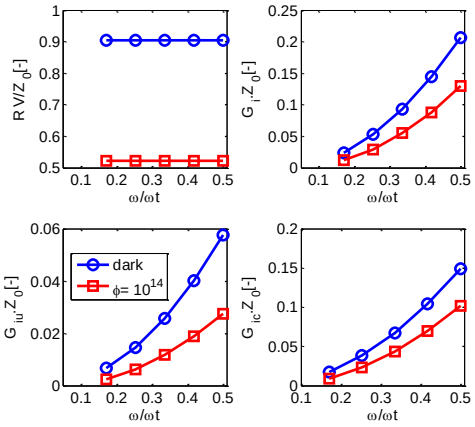

Figure 7: Correlation noise parameters

Figure 7 is the plot of corresponding correlation parameters (R_{va}), input-referred thermal noise current conductance (G_i), uncorrelated part of G_i (G_{iu}), and correlated part of G_i (G_{ic}). The value of correlation factor (c), which defines relationship between G_i, G_{ic} and G_{iu} remains almost constant. The input referred thermal noise conductance G_i is product of input referred noise resistance R_v and optimum noise admittance Y_{opt}. Since the noise resistance reduces under illumination, with Y_{opt} almost constant, G_i also decreases. This fall is reflected in G_{iu} and G_{ic}, thus signifying that corresponding noise correlation parameters also reduce with illumination.

Figure 8 is the plot of minimum noise figure in dark and with incident optical power at ω/ω_t=0.5. The minimum noise figure reduces under optical illumination with increasing power for optical flux density varying from Φ =1 x 10^{14} Wb/m^3 to Φ =1 x 10^{18} Wb/m^3. The reduction of minimum noise figure reduces under illumination indicates, the there is no additional noise contribution that the device adds to the signal reaching the load. This property can be used for design at RF.

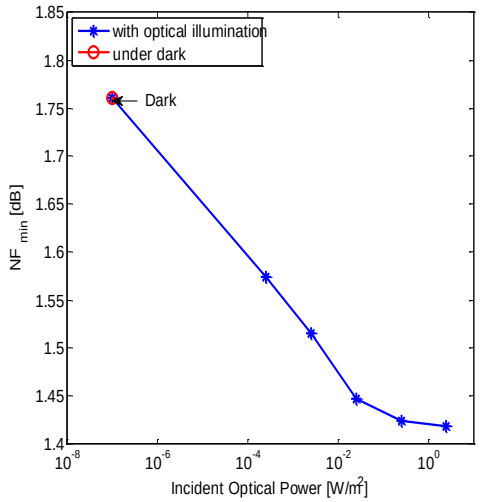

Figure 8: Noise figure with varying optical power

V. CONCLUSION

Computations and simulations for high frequency noise are carried out for optically illuminated silicon MOSFET at 300°K under dark and various illumination conditions. The noise model is developed and all four noise parameters are calculated. The corresponding noise parameters are also evaluated to have complete noise characterization. The reductions of noise parameters signify that the extra noise that the device adds to the signal reduces with optical illumination. Thus optical control of device assists in system design at high frequency where noise characteristics play an important role. The device also indicates that it is capability to function as a low noise photodetector for use in optical interconnects.

References

[1] "International Technology Roadmap for Semiconductors(Update Overview)," ITRS Report (2012).

[2] Jasprit Singh, *Semiconductor Optoelectronics*.: McGraw-Hill Inc, (1995).

[3] Prerana Jain, Mishra B.K., and Phade Gayatri, "AC performance of Optically Controlled MOSFET," in proc.of *IEEE Students Conference on Electrical, Electronics and Computer Sciences*, (2012.)

[4] M. Jamal Deen and Chiu-Hung, "MOSFET Modelling for Low Noise, RF circuit Design," in proceedings*Custom Integrated Circuits Conference*, 201,7467623,(2002).

[5] Christian C. Enz and Yuhua Cheng, "MOS Transistor Modeling for RF IC Design," *IEEE transactions on solid state circuits*, 35,186 (2000).

[6] P.Chakrabarti and Gopal I. V., "Charge-Sheet Model of a Proposed MISFET," P*hys. Stat.Sol*,28, 521–530, (1991).

[7] Dana Cristea, "Silicon Opto-FET for Photonic Integrated Circuits," in proc of International Symposium on Electron Devices for Microwave and Optoelectronic Applications, Vienna, 273,(2001)

[8] B.K. Mishra, "Computer Aided Modelling of Solid State Photo-detectors," Birla Institute of Technology, Ranchi, PhD thesis (1995).

[9] B.B.Pal and R.U.Khan Nandita Saha Roy, "Frequency–dependant characteristics of an ion–implanted GaAs MESFET with opaque gate under illumination," *Journal of Lightwave technology*, 18, 221, (2000).

[10] Joonho Gil, Seong-Sik Song, ,Jeonghu Han, Hyungcheol Shin, Choong-Ki Kim Kwangseok Han and Kwyro Lee, "Complete High-Frequency Thermal Noise Modeling of Short-Channel MOSFETs and Design of 5.2 GHz Low Noise Amplifier," *IEEE Journal Of Solid-State Circuits*, 40, 726,(2005).

[11] Luuk F. Tiemeijer, Ronald van Langevelde, Ramon J. HavensAdrie T. A. Zegers-van Duijnhoven Andries J. Scholten and Vincent C. Venezia, "Noise Modeling for RF circuit Simulation," *IEEE Transactions on Electron Devices*, vol. 50, no. 3, pp. 618-633, (2003)

[12] Yuhya Cheng, "MOSFET MODELING FOR RF IC DESIGN," *International Journal of High Speed Electronics and Systems*, vol. 11, no. 4, pp. 1007-1084, (2001)

[13] C Enz and A. Vittoz, *Charge-based MOS Transistor Modeling, The EKV model for low-power and RF IC design*, 1st ed. Wiltshire, UK: John Wiley and Sons, (2006).

[14] M. Jamal deen Yuhua Cheng and Chih-Hung Chen, "MOSFET Modelling for RF IC Design," *IEEE Transactions on Electron Devices*,52,1286, (2005).

[15] Prerana Jain and Mishra B.K., "An Invesigation of DC characteristics in Multifinger Optically Illuminated MOSFET," *International Journal of Computer Applications*,61, 12,(2013).

[16] Prerana Jain and Mishra B.K., "CV Investigation in Optically Illuminated MOSFET," *International Journal of Engineering Research and Applications* , 2, 1282,(2012).

APPENDIX A

This section presents the expressions for noise and its corresponding parameters. The small signal model parameters are evaluated from the charges in dark and under illumination. The resistances (R_G,R_{sub}), trans-conductances (g_m, g_{ms} *and* g_{mb}), capacitances (C_{gs}), transit frequency (f_T) for dark and under varying optical condition for the operating point of V_G= 1 V, V_D=1 V and V_B =0 V are evaluated in [3,15,16].

n:	Slope factor
v_{sat}:	Saturated drift velocity
L_{eff}:	Effective channel length
I_D:	Static drain current flowing into the drain terminal
R:	Equivalent substrate resistance
g_m :	Gate transconductance
g_{mb} :	Bulk transconductance
C_{gs} :	Total gate-to-source capacitance
ω_t :	Transit frequency
R_v :	Input-referred thermal noise voltage resistance
G_i :	Input-referred thermal noise current conductance
G_{iu} :	Uncorrelated part of G_i
G_{ic} :	Correlated part of G_i
Y_c :	Noise correlation admittance
G_c :	Noise correlation conductance
B_c :	Noise correlation susceptance
F :	Noise factor
NF :	Noise figure
F_{min} :	Minimum noise factor
NF_{min} :	Minimum noise figure
Y_{opt} :	Optimum source admittance for $F = F_{min}$
G_{opt} :	Optimum source conductance
B_{opt} :	Optimum source susceptance
c:	correlation factor

The slope factor η is given by

$$n = \frac{g_{ms}}{g_m} = \frac{g_{mb}}{g_m}$$

$$\Omega = \frac{\omega C_{gs}}{g_m}$$

$$\mathrm{B}_{sat} = \frac{\delta}{5n}$$

where δ is a bias dependant factor and taken as 4/3

$$\gamma_{sat}(i_f) = \gamma_{sat-long}\cdot\left(1 + \frac{1}{G(i_f)}\frac{v_{sat}.\tau_r}{L_{eff}}\right)$$

where $\gamma_{sat\text{-}long}$ = 2/3 for i_f >>1
= 1/2 for i_f <<1
v_{sat} is velocity at saturation taken as 1x 10^5 m/s
Γ_r is relaxation time taken as 1x 10^{-12} ps

$$G(i_f) = \frac{g_m.nU_T}{I_D}$$

$$\alpha_{sat} = n\gamma_{sat}$$

$$\alpha_g = \frac{g_m R_g}{\alpha_{sat}}$$

$$\alpha_{sub} = \frac{g_{mb} R_{sub}}{\alpha_{sat}}$$

$$\psi = 1 + \alpha_{sub} + \frac{\beta_{sat}}{\alpha_{sat}} + 2c_g\sqrt{\frac{\beta_{sat}}{\alpha_{sat}}}$$

$$\chi = 1 + \alpha_{sub} - c_g\sqrt{\frac{\partial}{5n\alpha_{sat}}}$$

$$R_v = \frac{\alpha_{sat}}{g_m}.D_c$$

$$G_i = \alpha_{sat} g_m \Omega^2.\psi$$

$$G_c = \frac{R_g.(g_m\Omega)^2.\Psi}{D_c}$$

$$B_c = \frac{g_m\Omega.\chi}{D_c}$$

$$D_c = 1 + \alpha_g + \alpha_{sub} + (g_m R_g\Omega)^2.\Psi$$
$$\cong 1 + \alpha_g + \alpha_{sub}$$

$$\Omega = \omega/\omega_t \approx \omega.\, c_{gs}/g_m$$

$$F_{\min} = 1 + 2R_v(G_{opt} + G_c)$$
$$= 1 + 2R_v.\left(\sqrt{G_{iu}/R_v + G_c^{\,2}} + G_c\right)$$

$$G_{opt} = \sqrt{\frac{G_{iu}}{R_v} + G^2{}_c} = \sqrt{G_i/R_v - B_c^{\,2}}$$

$$B_{opt} = -B_c$$

$$c = Y_c\frac{R_v}{G_i} = \frac{G_c + jB_c}{\sqrt{G^2{}_{opt} + B^2{}_{opt}}}$$

$$|c|^2 = \frac{G^2{}_c + B_c^{\,2}}{G^2{}_{opt} + B^2{}_{opt}}$$

$$G_{ic} = |c|^2 G_i$$

$$G_{iu} = (1 - |c|^2)\, G_i$$

.